Realistic Simulation of NSM-CFRP Strengthened T-Beam

Frank Ding, PhD

Simpson Strong-Tie

***Abstract**: This paper is a summary of finite element modeling approach used in the project for SC@UM Strengthening CFRP Challenge at FRPRCS-11. The modeling competition is to predict the behavior of a T-shaped reinforced concrete beam, shear and flexural strengthened with carbon reinforced polymer (CFRP) laminates according to the Near Surface Mounted (NSM) technique. A complete 3D Abaqus model was constructed to simulate the load displacement response of the CFRP laminates strengthened T-shaped reinforced concrete beam. Abaqus concrete damaged plasticity material model was employed to model concrete cracking/crushing failure. Embedded element was used to model concrete-rebar interaction. Cohesive zone model was used to simulate CFRP-concrete bonding behavior based on nonlinear mixed mode fracture of mode I and model II. A calibrated CFRP-concrete interface bond behavior based on published test data was conducted and the material parameters were subsequently applied in the simulation of the T-beam flexure test. Abaqus/Explicit solver was used to solve the complicated model on a 32-core high performance computing (HPC) Linux cluster. The presented approach has been proved to be very effective for the realistic simulation of FRP strengthened RC structure..*

***Keywords**: NSM, CFRP, Abaqus/Explicit, concrete damaged plasticity, cohesive zone model, nonlinear mixed mode fracture, HPC.*

1. Introduction

This paper is a summary of finite element modeling approach used in the project for SC@UM Strengthening CFRP Challenge at FRPRCS-11. The modeling competition is to predict the behavior of a T-shaped reinforced concrete beam, shear and flexural strengthened with carbon reinforced polymer (CFRP) laminates according to the Near Surface Mounted (NSM) technique.

The geometry of the T-beam cross-section is presented in Figure 1. The steel reinforcement arrangement is shown in Figure 1a. Both the longitudinal (3 laminates with 1.4x20 ⟦mm⟧^2 of cross section) and the transverse (2 laminates with 1.4x20 ⟦mm⟧^2 of cross section spaced at 300 mm) CFRP reinforcements inserted on the T-beam for flexural and shear strengthening are shown in Figure 1b.

The T-beam, simply supported, will be subjected to a non-symmetrical descending load P. The geometry of the T-beam, positioning of the supports and load P are presented in Figure 2. To simulate the service conditions and the corresponding loading, the T-beam will be subjected to an imposed deflection of L/350 at mid-span, where L is the distance between supports, at a deflection rate of 20 µm/s. Subsequently, the T-beam will be instantly unloaded and the transverse and longitudinal CFRP laminates will be applied according to the NSM strengthening technique. No further measures to obliterate the produced cracking will be undertaken. Finally, the retrofitted T-beam will be tested under displacement control up to failure at a displacement rate of 20 μm/s. The load-deflection response will be recorded and the evolution of the deformation of the T-beam during testing will be documented. The crack patterns observed at the T-beam surface will be also documented by a sequence of images.

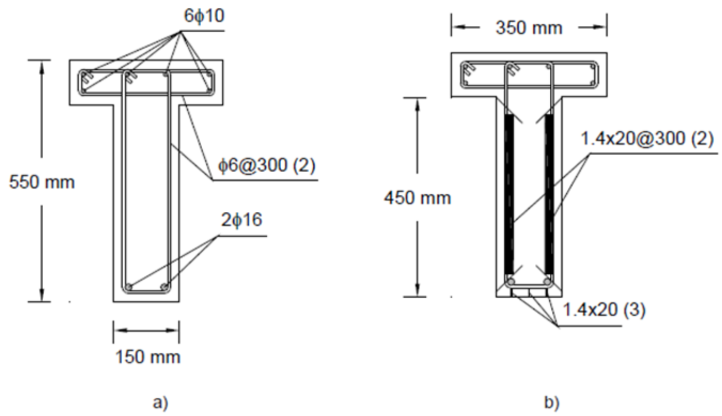

Figure 1. T-beam cross section geometry, a) before and b) after CFRP laminate strengthening

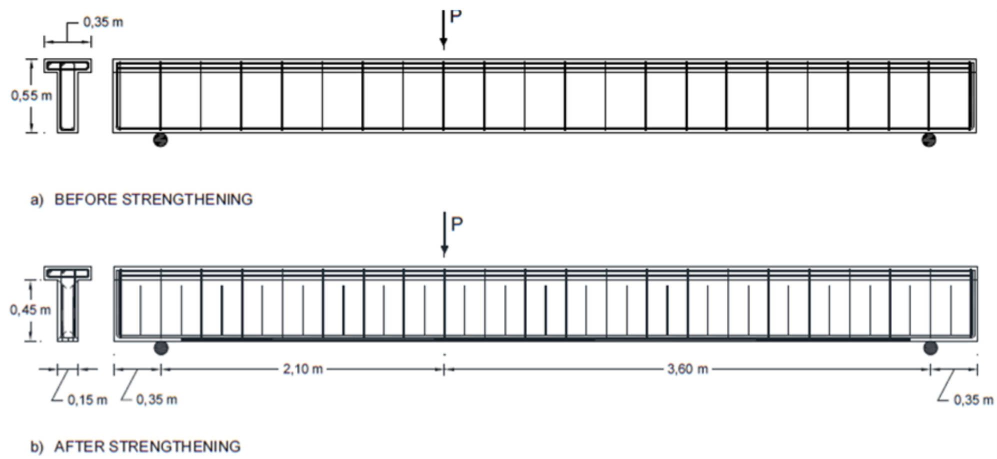

Figure 2. T-beam geometry and steel reinforcement, a) before and b) after CFRP laminate strengthening

2. Material model

There are steel reinforcement, concrete, CFRP laminates, and epoxy adhesive used in the specimen construction. The material characterization was done at UM (University of Minho), and the material data was provided in the document (SC@UM, 2013). The material models used in simulation are listed in the following sections.

2.1 Steel reinforcement

Bi-linear elastic-plastic isotropic model was used to model the steel reinforcement bars. A Poisson's ratio of 0.3 was used for the steel reinforcement. The bond between steel reinforcement and concrete was assumed as a perfect bond. Table 1 shows the material parameters used for the steel bars.

Table 1 – Material Parameters for Steel Bars.

Diameter	E_s(GPa)	F_{sy}(MPa)	F_{su}(MPa)
6 mm	211.53	552.59	679.64
10 mm	205.81	529.36	624.58
16 mm	207.19	552.76	657.45

Note: E_s = steel Young's modulus; F_{sy} = steel yield stress; F_{su} = steel tensile strength

2.2 Concrete

Concrete damaged plasticity model in Abaqus (SIMULIA, 2012) was used to model the concrete behavior. This model assumes that the main two failure modes are tensile cracking and compressive crushing. Under uni-axial tension, the stress–strain response follows a linear elastic relationship until the value of the failure stress is reached. The failure stress corresponds to the onset of micro-cracking in the concrete material. Beyond the failure stress the formation of micro-cracks is represented with a softening stress–strain response. Hence, the elastic parameters required to establish the first part of the relation are elastic modulus E_c, and tensile strength f_{ct}. The compressive behavior in 28 days testing data from (SC@UM, 2013) were used for E_c to be 35.77 GPa, and the compressive strength f_{cu} to be 24.51 MPa. f_{ct} was then calculated by Equation 1:

$$f_{ct} = 0.33\sqrt{f_{cu}} = 1.63\ MPa \quad (1)$$

To specify the post-peak tension failure behavior of concrete the fracture energy method was used. The fracture energy G_f which is the area under the softening curve, and was assumed to be 70 N/m according to the reported maximum aggregate size of 15mm (SC@UM, 2013). Poisson's ratio for concrete was assumed to be 0.2.

2.3 CFRP Laminates

Considering that the response of the CFRP laminates in tension is elastic until the tensile strength is reached and that failure is purely brittle, the tensile response is entirely described by the Young's modulus of 171.63 GPa and the tensile strength of 2534.03 MPa. The failure strain is 0.01478 (SC@UM, 2013). Isotropic linear elastic model with strain failure was used for the CFRP laminates.

2.4 Adhesive

Adhesive was assumed to isotropic elastic-perfectly plastic material. The Young's modulus is 7.66 GPa, and the yield stress is 20.72 MPa based on (SC@UM, 2013).

3. Finite element model

A realistic 3D finite element model was constructed to simulate the testing configuration and loading. Solid element 10-noded tetrahedral element C3D10M was used for concrete. Beam element B31 was used for steel reinforcing bars. 8-noded reduced integration hex element C3D8R was used to model epoxy adhesive. CFRP laminate was modeled using continuum shell element SC8R. The roller bearing bar support was modeled as rigid elements.

3.1 Interactions and constraints

Abaqus/explicit general contact was used to model all contact situations. Concrete-adhesive interface was modeled using Abaqus tie constraint. Rebar modeling used Abaqus embedded element technique (SIMULIA, 2012). Rebar beam elements were embedded in the concrete solid host elements, and a perfect bonding interaction was assumed. Adhesive-CFRP laminate interface was modeled using Abaqus surface-based cohesive behavior. Abaqus surface-based cohesive behavior features allow the specification of generalized traction-separation behavior for surfaces. This behavior offers capabilities that are very similar to cohesive elements that are defined using a traction-separation law (SIMULIA, 2012). However, surface-based cohesive behavior is typically easier to define and allows simulation of a wider range of cohesive interactions.

3.2 CFRP-adhesive interface

Concrete-adhesive interface was modeled as a perfect bond using Abaqus tie constraint. The CFRP laminate–adhesive interface was modeled using Abaqus surface-based cohesive behavior based on traction-separation law. Figure 3 shows a graphic interpretation of a simple bilinear traction-separation law written in terms of the effective traction τ and effective opening displacement δ. The interface is modeled as a rich zone of small thickness and the initial stiffness K_0 is defined as Equation 2 (Obaidat, 2010):

$$K_0 = \frac{1}{\frac{t_i}{G_i} + \frac{t_c}{G_c}} \qquad (2)$$

where t_i is the adhesive thickness, t_c is the concrete thickness, and G_i and G_c are the shear modulus of adhesive resin and concrete respectively. The values used for this study were t_i = 1.7 mm, t_c = 5 mm, G_i = 2.95 GPa, and G_c = 10.8 GPa. Thus K_0 = 0.962 GPa.

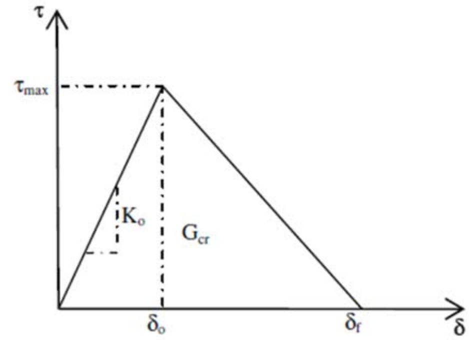

Figure 3. Bilinear traction–separation constitutive law.

From Figure 3, it is obvious that the relationship between the traction stress and effective opening displacement is defined by the stiffness K_0, the local strength of the material τ_{max}, a characteristic opening displacement at fracture, δ_f, and the energy needed for opening the crack, G_{cr}, which is equal to the area under the traction–displacement curve. The maximum bond shear stress, τ_{max}, was initially set to 18.1 MPa based on CFRP-concrete interface bond experiment by (Sena Cruz, 2006), then numerically calibrated to the pullout-bending test data from (Sena Cruz, 2006).

For fracture energy G_{cr}, the value of 90 N/m was used based on the previous study by (Obaidat, 2010).

The initiation of damage was assumed to occur when a quadratic traction function involving the nominal stress ratios reached the value one. This criterion can be represented by (SIMULIA, 2012):

$$\left(\frac{\sigma_n}{\sigma_n^0}\right)^2 + \left(\frac{\tau_s}{\tau_s^0}\right)^2 + \left(\frac{\tau_t}{\tau_t^0}\right)^2 = 1 \tag{3}$$

where σ_n is the cohesive tensile and τ_s and τ_t are shear stresses of the interface, and n, s, and t refer to the direction of the stress component. The values used for this simulation were $\sigma_n^0 = 41$ MPa, and $\tau_s^0 = \tau_t^0 = 34$ MPa. Interface damage evolution was expressed in terms of energy release. The description of this model is available in the Abaqus material library (SIMULIA, 2012). The dependence of the fracture energy on the mode mix was defined based on the Benzaggah–Kenane fracture criterion (SIMULIA, 2012). Benzaggah–Kenane fracture criterion is particularly useful when the critical fracture energies during deformation purely along the first and the second shear directions are the same; i.e., $G_s^c = G_t^c$. It is given by (SIMULIA, 2012):

$$G_n^c + (G_s^c - G_n^c)\left(\frac{G_\varphi}{G_J}\right)^\eta = G^c \tag{4}$$

where $G_\varphi = G_s + G_t$ and $G_J = G_n + G_s$; and η are the material parameter.

G_n, G_s and G_t refer to the work done by the traction and its conjugate separation in the normal, the first and the second shear directions, respectively. The values used for this analysis were $G_n^c =$ 9N/m, $G_s^c = 90$N/m, and $\eta = 1.45$.

3.3 CFRP-concrete bond behavior calibration

(Sena Cruz, 2006) pullout-bending test data from fcm40_Lb120_M was used to calibrate the surface-based cohesive contact behavior parameters. Pullout-bending test setup was shown in Figure 4. Abaqus/Explicit model was constructed to simulate the pullout-bending test to get the CFRP-concrete bond pullout force and slip response to compare with the result in (Sena Cruz, 2006).

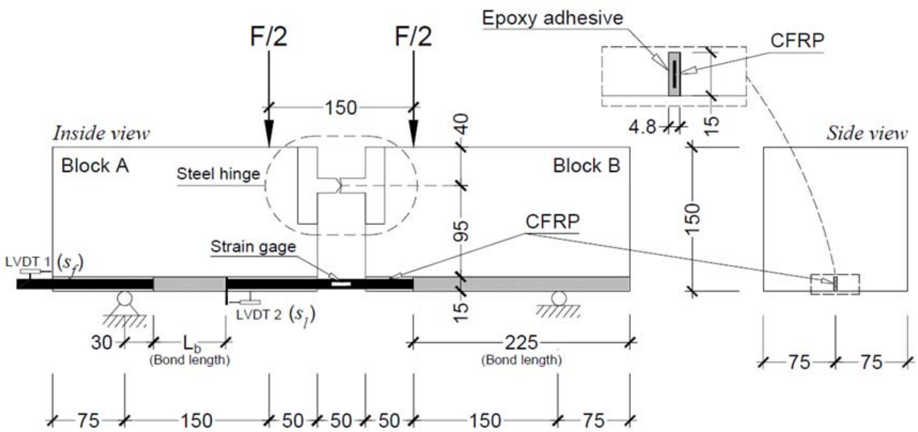

Figure 4. Pullout-bending test configuration from (Sena Cruz, 2006)

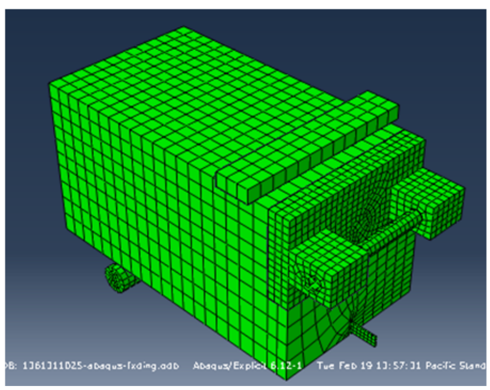

Figure 5. 3D Abaqus pullout-bending test model

Several numerical iterations were conducted to fine tune the Abaqus CFRP-concrete bond material parameters. The final predicted bond pullout force was 27.9 kN from the Abaqus model, where (Sena Cruz, 2006) result was 27.7 kN. The fitted surface-based cohesive contact material parameters were used in the T-beam CFRP bond behavior modeling for the competition.

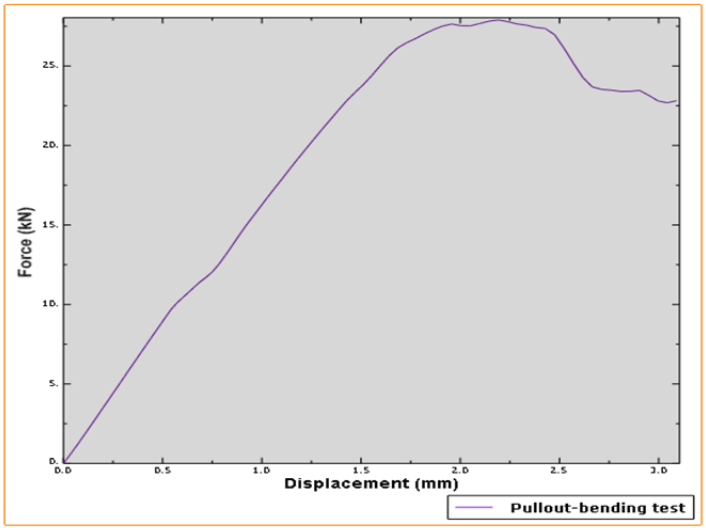

Figure 6. Pullout-bending CFRP pullout force vs. slip

4. Results

A complete 3D Abaqus model was constructed using Abaqus/CAE. Figure 7 shows the T-beam model with reinforcing steel bars, CFRP strips, adhesive, and steel roller supports visible through model translucency. Abaqus/Explicit was employed to solve the model on a 32-core Linux cluster because of the model size and progressive damage and failure mechanism involved. The job run time was close to 5 hours.

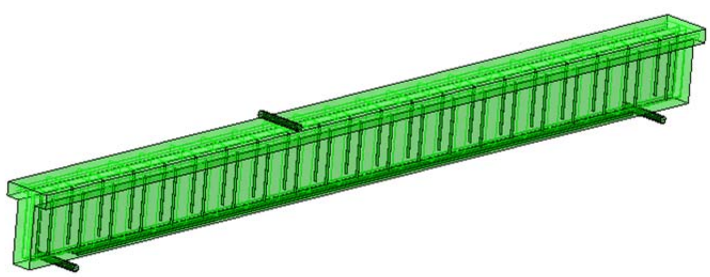

Figure 7. T-beam model built in Abaqus/CAE

T-beam pre-loading was simulated without CFRP strengthening. Figure 8 shows the load-deflection curve compared with the test result. The predicted load was higher than the test after the initial stiffness. This is due to the fact that a perfect bond model was assumed for rebar reinforcement inside the concrete. Figure 9 shows T-beam crack patterns. The predicted crack patterns closely resemble those found in the test.

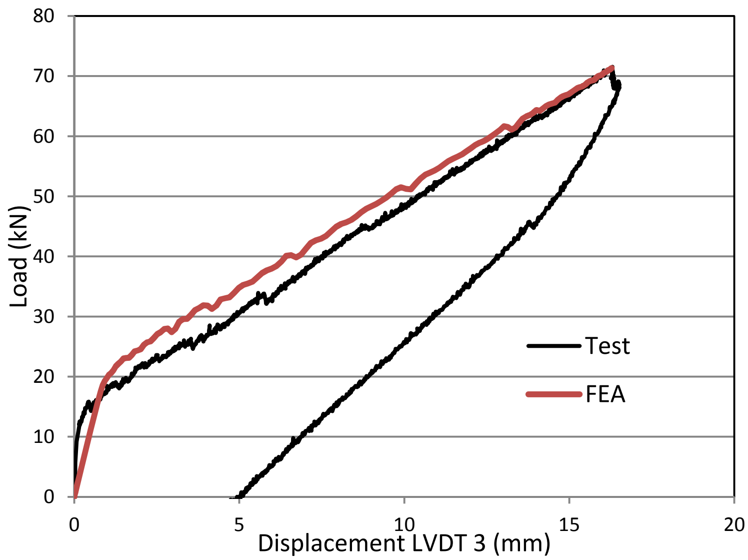

Figure 8. Load displacement response of the T-beam before CFRP strengthening

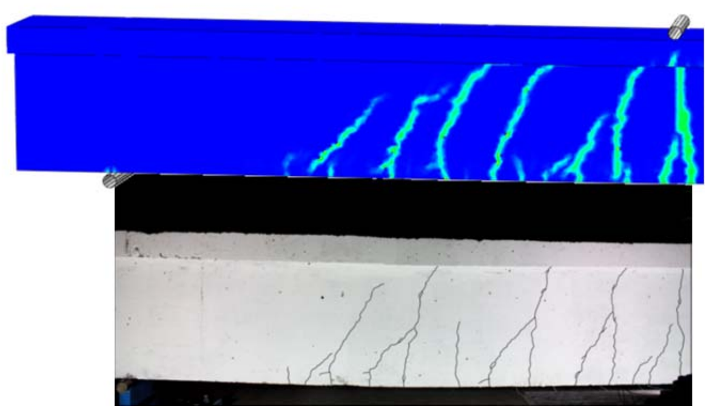

Figure 9. Crack patterns of the T-beam Test vs. FEA before CFRP strengthening

Figure 10 shows final T-beam load displacement curve after CFRP strengthening. Based on the final test data feedback from the competition organizer, two material parameters were updated (concrete strength of 31.26MPa at 99 day and tested adhesive strength of 28.16MPa) and a re-run was initiated for the analysis. Nothing in the model was changed other than updating the two material parameters. The peak load was predicted to be 140.31kN at the deflection of 60.2mm. The test result showed a peak load of 145.7kN at the deflection of 60.1mm. The predicting error is about -3.7%, which is in good agreement with the test result.

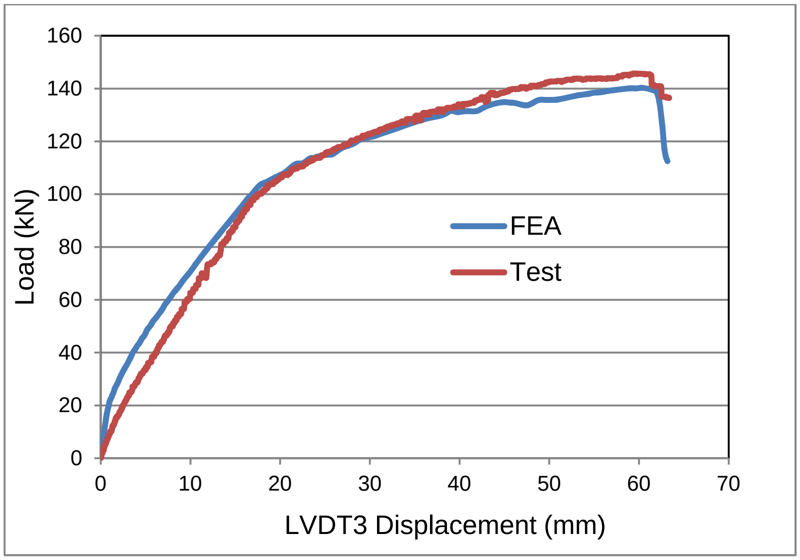

Figure 10. The predicted T-beam load displacement curve FEA vs. Test for retrofitted beam

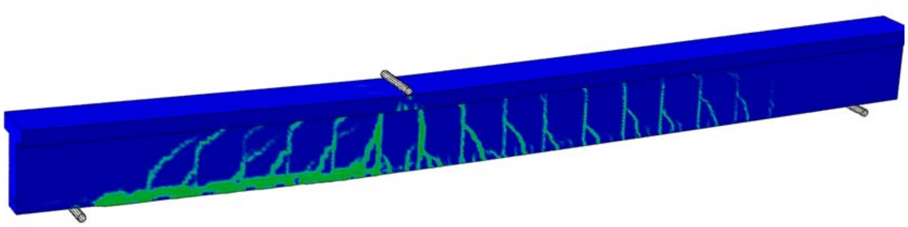

Figure 11. T-beam crack patterns at peak load for retrofitted beam

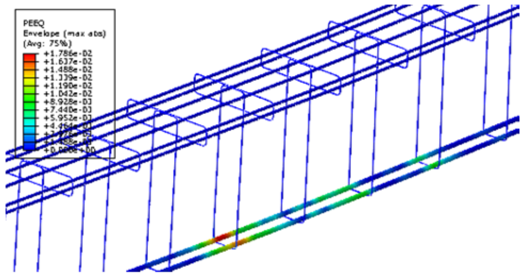

Figure 12. Steel reinforcing bars plastic strain in the loaded section at peak load

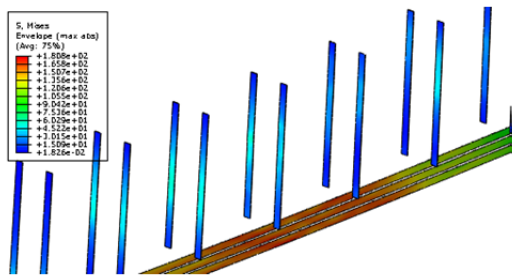

Figure 13. CFRP laminates von Mises stress in the loaded section at peak load

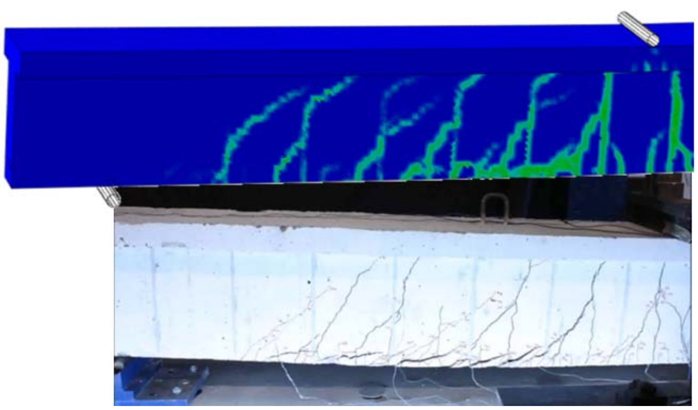

Figure 14. CFRP de-bonding and concrete crack patterns at peak load Test vs. FEA for retrofitted beam

At the peak load, the CFRP laminates' maximum strain is 0.011 and maximum stress is 2.05 GPa. The maximum plastic strain at the bottom steel reinforcing bars is 0.0216. The failure is predicted to be the CFRP-concrete de-bonding failure, then T-beam bottom concrete cracking failure. Figure 14 shows concrete crack patterns comparison of test and FEA at peak load.

5. Conclusion

A complete 3D finite element model was constructed to simulate the load displacement response of the CFRP laminates strengthened T-shaped reinforced concrete beam according to the Near Surface Mounted (NSM) technique. A calibrated CFRP-concrete interface bond behavior based on published test data was conducted and the material parameters were subsequently applied in the simulation of the T-beam flexure test. The predicted result in terms of peak load and failure mode shows a very good agreement between test and 3D finite element model. The 3D modeling approach could be adopted to realistically model NSM-CFRP strengthened RC structures with the computing power of the Linux-based HPC clusters.

6. Acknowledgement

I would like to express my sincere appreciation to the SC@UM Challenge organizing committee at FRPRCS-11 for letting me participate in this competition.

7. References

1. Obaidat Yasmeen Taleb, Heyden, Susanne, Dahlblom, Ola, "The effect of CFRP and CFRP/concrete interface models when modeling retrofitted RC beams with FEM", Composite Structures, Vol. 92, No. 6, May 2010, pp. 1391-1398.
2. Sena Cruz, J., Barros, J., Gettu, R., and Azevedo, Á, "Bond Behavior of Near-Surface Mounted CFRP Laminate Strips under Monotonic and Cyclic Loading", Journal of Composites for Construction, Vol. 10, No. 4, August 2006, pp. 295-303.
3. SC@UM, "Characteristics of the Materials", Strengthening CFRP Challenge at University of Minho FRPRCS-11, April 2013.
4. SIMULIA, "Abaqus Analysis User's Manual", Abaqus 6.12 Documentation Collection, Dassault Systèmes, 2012